Degenerate bound states in the continuum in square and triangular open acoustic resonators

Almas Sadreev [ORCID],[1,*] Evgeny Bulgakov [ORCID],[1] Artem Pilipchuk,[1] Andrey Miroshnichenko,[2] and Lujun Huang[2]

[1]*Kirensky Institute of Physics Federal Research Center KSC SB RAS Krasnoyarsk 660036, Russia*

[2]*School of Engineering and Information Technology, University of New South Wales Canberra, Northcott Drive, AC, 2600, Australia*

We consider square and equilateral triangular open acoustic resonators with the C_{4v} and C_{3v} symmetries, respectively. There is a unique property of square and triangular resonators of accidental number fourfold degeneracy of eigenstates that gives rise to twofold-degenerate Friedrich-Wintgen (FW) bound states in the continuum (BICs). Compared to usual FW BICs, the degenerate FW BICs maintain high Q factor in wide range of the size of resonators. That removes the fabrication difficulties of the proper choice of resonator. The presence of degenerate BICs in triangular resonators is extremely sensitive to switch output flows by small perturbations with 100% efficiency.

I. INTRODUCTION

A new paradigm for the trapping and confining of resonant modes has emerged in recent years based on the bound states in the continuum (BICs) in wave systems. BICs, also known as trapping mode with infinite large Q factor, have triggered extensive interest in photonic and acoustic communities [1–5]. The most straightforward mechanism of BICs is the symmetrical incompatibility of closed system states with propagating states of the continuum [6–10]. More interesting, Friedrich-Wintgen (FW) BICs are the result of full destructive interference of two or more resonant modes competing for leakage into open channels of waveguides [4,11,12]. The FW BICs can be realized in open resonators by a gradual change of aspect ratio of the resonator when a degeneracy of eigenfrequencies occur [12]. In acoustic systems, the FW BICs were considered by many scholars [13–17]. The experimental evidence for the FW BICs was reported by Lepetit and Kanté [18] and by Huang *et al.* [19] in the most straightforward configuration of rectangular resonator opened to attached waveguide.

Although the last time BICs had been successfully demonstrated in different acoustic resonators fabricated by 3D printing, the Q factor of quasi-BICs was sensitive to the structure imperfections. Moreover, continual variation of the aspect ratio of the resonator for the achievement of FW BICs is very challenging for any type of resonator, acoustic, metallic, or dielectric. Therefore, a search of FW BICs not sensitive to the aspect ratio of resonators is highly desired. In the present paper, we advocate square or equilateral triangular resonators with the group symmetries C_{4v} and C_{3v}, respectively. Its eigenmodes ψ_{mn} and eigenfrequencies ν_{mn}^2 exhibit trivial degeneracy by permutation of indices $m \leftrightarrow n$. Here the eigenfrequencies are given in terms of the frequency $\omega_0 = \pi s/a$, where s is the velocity of sound or light in air, and a is the side size of the resonator. Therefore, one can expect that opening of the resonator by attachment of waveguides transforms these degenerate eigenmodes into superradiant mode and FW BIC

for granting as it follows from the FW mechanism of BICs, which occur at degeneracy of eigenfrequencies [4,11,12,20]. Variants of attachment of waveguides to a square resonator are sketched in Fig. 1. However, for the case (a) in Fig. 1 the FW BICs occur only after deformation of square resonator into the rectangular one [19]. The reason for cancellation of FW BICs is lowering of the symmetry C_{4v} of closed square resonator towards C_{2v} after the (a) case opening. Quantitatively, the coupling of eigenmodes of a square resonator with evanescent modes of waveguides perturbs the eigenfrequencies of the resonator and removes the permutation degeneracy of the open square resonator [21]. Next, consider the cases in which for opening of the resonators the symmetry C_{4v} is preserved, as sketched in Fig. 1(b) and 1(c). In this case the degenerate eigenmodes (m, n) and (n, m) of closed resonator and their resonant counterparts of open resonator are both classified according to the different irreducible representations of the group C_{4v} and therefore can not be coupled via the continuum of waveguides that cancels the FW mechanism of the BICs too. The same consideration is applied to equilateral triangular resonator with the symmetry group C_{3v}.

However, there is a unique case of accidental or number degeneracy of eigenmodes over twofold in the square and equilateral triangle $\nu_{mn}^2 = \nu_{m'n'}^2$. For example, in square acoustic resonator two choices of integers $m = 1$, $n = 6$ and $m' = 5$, $n' = 4$ have the same frequency $25/a^2$ [22,23]. That brings fourfold degeneracy of a closed resonator that plays the key role in the existence of twofold degeneracy of the FW BICs provided that open resonators preserve the group symmetries C_{4v} or C_{3v} as shown in Fig. 1(b)–1(d). We show that the degenerate FW BICs are classified according to the two-dimensional irreducible representation E of these group symmetries. Without loss of generality we focus on the acoustic resonators with Neumann boundary conditions in which BICs can be directly probed by microphone measurements of acoustic pressure inside resonators [17,19]. Actually, resonators are three dimensional, but the acoustic resonators allow completely disregard the third dimension if the thickness of the resonator is small enough compared to longitudinal sizes as sketched in Fig. 1(d). In that case, the solutions are

---

*Corresponding Author: almas@tnp.krasn.ru
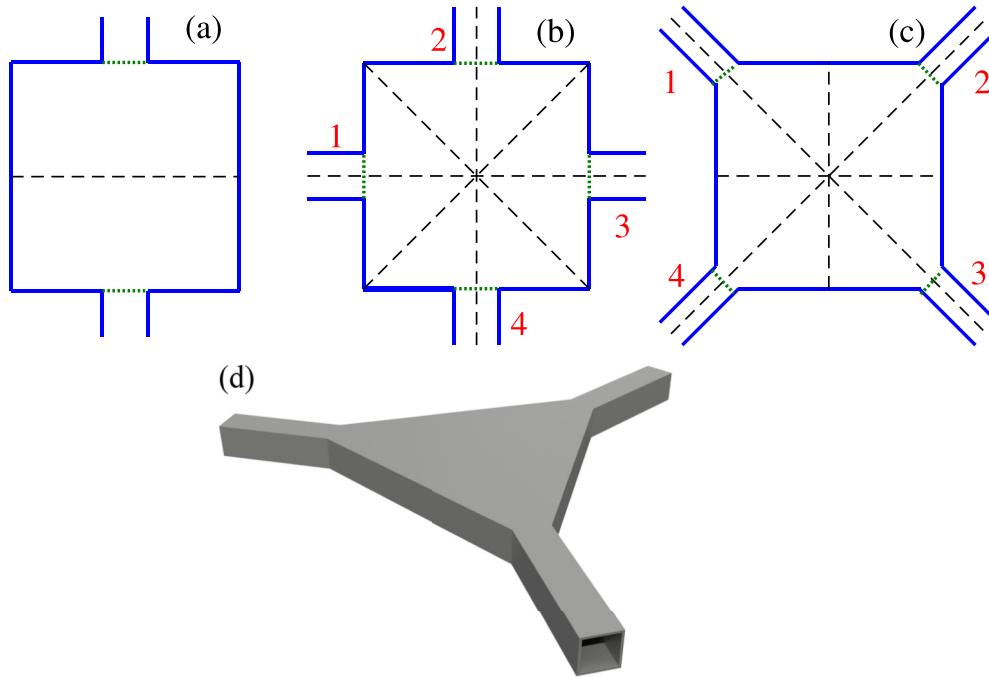
FIG. 1. (a) Two waveguides attached to the square resonator with the symmetry C_{4v} lower the symmetry of the open system until inversion symmetry σ. (b) and (c) Four identical waveguides attached to square resonator preserve the symmetry C_{4v}. (d) Three waveguides attached to equilateral triangle resonator preserve the symmetry C_{3v}.

constant over the third dimension to be excluded from the solutions presented in the Appendix. That opens many ways for experimental verifications of theoretical predictions outlined below in the square and equilateral triangle resonators.

II. THE SP BICS DUE TO PERMUTATION SYMMETRY IN OPEN SQUARE RESONATORS

The symmetry of the open resonators is important for classification and establishment of BICs. For dielectric resonators embedded into radiation space, the total symmetry is given by the structure that determines multipole classification of radiation and the symmetry of ultrahigh Q resonances (quasi-BICs) of the structure consisting of one or a few symmetrical dielectric cavities [24–26]. The symmetry of BICs in photonic crystals is given by the symmetry of the crystals [27–30]. As opposed to the above, the symmetry of resonators with attached directional waveguides is determined by the compatibility of the symmetry of closed resonators with the symmetry of waveguides. The symmetry of the total system can be lowered or can coincide with the symmetry of closed resonators as illustrated in Fig. 1.

The eigenmodes and eigenfrequencies of the acoustic square resonator are collected in the Appendix. There are two distinct pairs of degenerate states $\psi_{m,n}, \psi_{n,m}, m \neq n$. The first pair of the eigenmodes with $m - n$ odd is classified according to the two-dimensional irreducible representation E. The particular case of $m = 2, n = 3$ is demonstrated in Fig. 6 in the Appendix. The second pair with $m - n$ even is

classified according to the reducible representations. Only the linear combinations $\psi_{m,n} \pm \psi_{n,m}$ are classified according to the irreducible one-dimensional representations B_1 and A_1 or B_2 and A_2 respectively. A particular case of eigenmodes ψ_{24} and ψ_{42} classified according to B_2 and A_2 is shown in Fig. 7 in the Appendix.

Opening the resonator transforms the real eigenfrequencies of the closed resonator into the complex eigenfrequencies. The procedure of transition from a closed system to an open system can be performed by use of the Feshbach projection technique that results in the non-Hermitian effective Hamiltonian [31–36]. The complex eigenvalues of this Hamiltonian respond to the position of resonances and resonant line widths and therefore provide an excellent way to establish BICs as eigenmodes of effective Hamiltonian with real eigenvalues [4]. The specific form of the effective non-Hermitian Hamiltonian is given in the Appendix and is applied to open acoustic resonators [36].

Let us first consider the degenerated pair of eigenmodes of closed square resonator $\psi_{m,n}, \psi_{n,m}$ with $m - n$ odd and $m \neq n$ classified according to the two-dimensional representation E, for example, the pair presented in the Appendix ψ_{23} and ψ_{32}. The coupling matrix elements of these modes with the first open channel $p = 1$ and the second closed channel $p = 2$ for the case in Fig. 1(b) are collected in the Appendix. As a result, we can write the effective non-Hermitian Hamiltonian projected into these modes whose general form is given in Eq. (A3) of the Appendix

$$\widehat{H}_{\text{eff}} = \begin{pmatrix} 5/a^2 - 2ik_1|k_2|\alpha^2 + 2|k_2|\beta^2 & 0 \\ 0 & 5/a^2 - 2ik_1|k_2|\alpha^2 + 2|k_2|\beta^2 \end{pmatrix}. \tag{1}$$
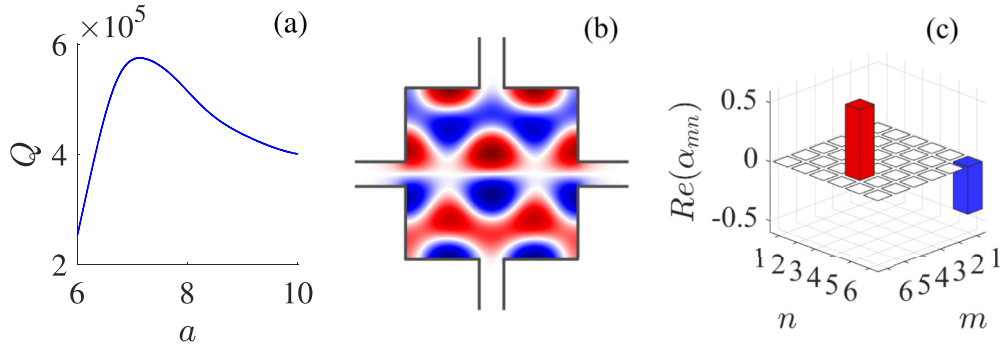
FIG. 2. (a) The Q factor of quasi-FW BIC shown in subplot (b) with the modal expansion coefficients shown in (c).

Here, according to Table II of the Appendix, we introduced the notations $\alpha = W_{2,3;p=1,C=1} = -\frac{2}{\pi}\sin\frac{\pi}{a}$, $\beta = W_{2,3;p=2,C=1} = f(a)$. The case of Fig. 1(c) gives the similar diagonal matrix

$$\widehat{H}_{\text{eff}} = \begin{pmatrix} 5/a^2 - 4ik_1|k_2|\gamma^2 + 4|k_2|\delta^2 & 0 \\ 0 & 5/a^2 - 4ik_1|k_2|\gamma^2 + 4|k_2|\delta^2 \end{pmatrix}. \tag{2}$$

Here, the coupling strengths γ and δ can be evaluated only numerically by integration over thin dotted lines shown in Fig. 1(c). Irrespectively, we obtain that the degenerate pair of eigenmodes $\psi_{2m,2n+1}$ and $\psi_{2n+1,2m}$ transforms into two degenerate resonances but not BICs. That has a clear physical origin. Since the symmetry of the open resonator C_{4v} is preserved, the eigenmodes of the closed resonator $\psi_{2,3}$ and $\psi_{3,2}$ are modified but cannot be coupled through the open continuum $p = 1$ of waveguides owing to the symmetry C_{4v} of the open square resonator. As a result, the FW mechanism of BICs is canceling.

Next, we consider the pair $\psi_{s,a} = \psi_{m,n} \pm \psi_{n,m}$, $m \neq n$ and $m - n$ even, which are classified according to the one-dimensional irreducible representations B_2 and A_2. Examples of these eigenfunctions $m = 2$, $n = 4$ are illustrated in Fig. 7 of SI. For the case in Fig. 1(b), all coupling matrix elements with the first open channel of each waveguide equal zero as clearly seen in Fig. 7 of SI. As a result, only closed channels of waveguides contribute in the effective Hamiltonian, which in the space of the eigenmodes $\psi_{2,4}$ and $\psi_{4,2}$ takes the following form:

$$\widehat{H}_{\text{eff}} = \begin{pmatrix} 10/a^2 + 4|k_2|(b(a)^2 + c(a)^2) & -4|k_2|b(a)c(a) \\ -4|k_2|b(a)c(a) & 10/a^2 + 4|k_2|(b(a) + c(a)^2) \end{pmatrix}. \tag{3}$$

Therefore, we have two SP BICs $\psi_{s,a}$ shown in Fig. 2 of SI with the eigenfrequencies

$$\nu_{s,a}^2 = 10/a^2 + 4|k_2| \begin{cases} b(a)^2 \\ c(a)^2 \end{cases}, \tag{4}$$

where the coupling constants $b(a), c(a)$ are collected in Eq. (A9) of SI.

III. THE TWO-FOLD DEGENERATE BICS IN OPEN SQUARE RESONATOR

As said in the Introduction there is the accidental number degeneracy of two doublets each degenerated by permutation of indices. For example, eigenmodes with indices 1, 6 and 4, 5, both classified according to the two-dimensional irreducible representation E, have the same eigenvalue $\nu_{16}^2 = \nu_{4,5}^2 = 25/a^2$. The next quartet of degenerated eigenmodes is, for example, 3, 10, 10, 3 and 7, 8, 8, 7 with the eigenvalue $85/a^2$. It is reasonable to project the effective non-Hermitian Hamiltonian onto this space of the eigenmodes. Let us enumerate the eigenmodes as follows:

$$\phi_1 = \psi_{1,6}, \phi_2 = \psi_{5,4}, \phi_3 = \psi_{6,1}, \phi_4 = \psi_{4,5}.$$

In order to close the second channel $p = 2$ of waveguides, we consider the eigenfrequencies of the resonator below the second cutoff of the waveguide, i.e., $\nu_{m,n}/a < 1$ if to express side sizes of resonators a via the width of waveguides $d = 1$. In particular, for the eigenstates under consideration the size of resonator is to exceed $a > 5$.

Let us first consider the case of sidewall connection of waveguides as shown in Fig. 1(b). The coupling matrix elements of these eigenmodes with open channel $p = 1$ and closed channel $p = 2$ are collected in Tables II and III of the Appendix. As a result, we obtain for the effective Hamiltonian in truncated Hilbert space of the eigenfunctions ϕ_j, $j = 1, 2, 3, 4$

$$\widehat{H}_{\text{eff}} = \frac{1}{a^2}\begin{pmatrix} \hat{h}_{\text{eff}} & 0 \\ 0 & \hat{h}_{\text{eff}} \end{pmatrix},$$

$$\widehat{h}_{\text{eff}} = \begin{pmatrix} \epsilon - i\gamma_1 & -u - i\sqrt{\gamma_1\gamma_2} \\ -u - i\sqrt{\gamma_1\gamma_2} & -\epsilon - i\gamma_2 \end{pmatrix}, \tag{5}$$

where according to Tables II and III in the Appendix

$$\epsilon = |k_2|(g(a)^2 - h(a)^2), \quad u = 2|k_2|g(a)h(a), \quad \gamma_1 = \frac{4k_1}{a^2}, \quad \gamma_2 = \frac{2k_1}{\pi^2}\sin^2\left(\frac{2\pi}{a}\right), \tag{6}$$

and according to Eq. (4) in the Appendix $k_1 = \nu = \nu_{16} = 5/a$, $|k_2| = 7/a$.

One can see that the effective Hamiltonian consists of two identical blocks 2×2, each of which has typical form for
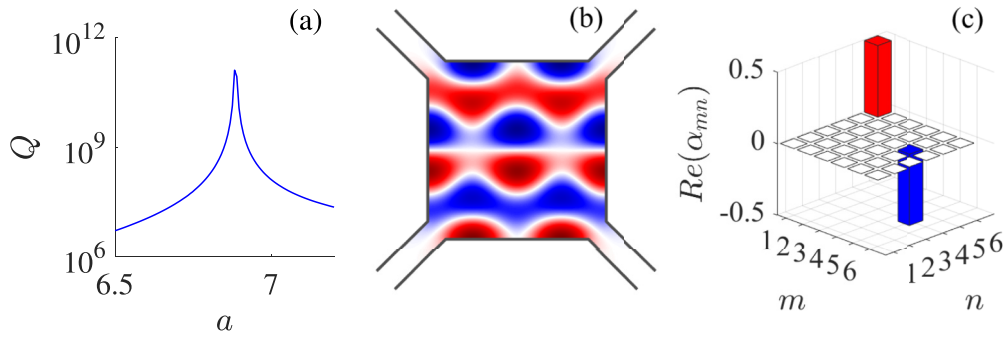
FIG. 3. The same as in Fig. 2 but for vertex connection of resonator to waveguides as shown in Fig. 1(c).

description of FW BICs [4,11,20]. Comparison with expressions (1) and (3) shows that the eigenmodes $(1, 6)$ and $(5, 4)$ and, respectively, $(6, 1)$ and $(4, 5)$ are coupled through the continuum of waveguides that gives rise to FW mechanism of two degenerate BICs classified according to the two-dimensional irreducible representation E. If we neglected by closed channel, $p = 2$, one could have two degenerate FW BICs for $a > 5$. However, the evanescent modes of waveguides play the principal role because they give rise to real coupling u between modes. For $u \neq 0$, the FW BIC occurs in the framework of the Hamiltonian (5) according to the following equation [4,20,37]:

$$u(\gamma_1 - \gamma_2) = 2\epsilon \sqrt{\gamma_1 \gamma_2}. \tag{7}$$

It is easy to fulfill Eq. (7) if the parameters $u, \gamma_1, \gamma_2, \epsilon$ were independent. However, for the present case all constants depend on only the square size a as given in Eq. (6). As Comsol MultiPhysics shows in Fig. 2(a) the condition (7) is not fulfilled for variation a that defines the solution as quasi-FW BIC although with extremely large Q factor around 600 000. In view material losses of 3D printed acoustic resonators which restrict the Q factor by order of 10^3 [19] one can consider the solution in Fig. 2(b) as the FW BIC. Remarkably, compared to usual FW BICs with sharp peak in the Q factor for variation of the sizes of resonator the degenerate FW BICs maintain extremely high Q factor in wide range of the size. That relieves experimentalists from the fabrication difficulties of proper choice of the resonators.

Figure 2(c) clearly shows that this BIC is composed of eigenmodes $(1, 6)$ and $(5, 4)$. The FW BIC composed of the eigenmodes $(6, 1)$ and $(4, 5)$ differs from this solution by 90 °°degree rotation.

In order to restore true degenerate FW BICs, we attach waveguides at the vertices of the square as shown in Fig. 1(c) which also give equal couplings of eigenmodes of the square resonator with the continua of waveguides. However similar to side coupling of square with waveguides the evanescent modes remove the number degeneracy of modes $1, 6$ and $5, 4$. Numerics reveals two degenerate FW BICs with the frequency $\nu = 0.832051$ occur for variation of square size $a = 6.8818$, the first of which is shown in Fig. 3. One can see that FW BIC is superposed of two eigenmodes $(1, 6)$ and $(5, 4)$. The second degenerate FW BIC is obtained by 90° rotation and both BICs are classified according to the two-dimensional representation E.

IV. DEGENERATE BICS IN EQUILATERAL TRIANGLE

Less obvious cases of the number degeneracy exist in the equilateral triangle with the eigenmodes and eigenfrequencies presented in the Appendix. Similar to a square resonator, all eigenmodes are twofold degenerate relative to $m \leftrightarrow n$, giving rise to the FW BICs. However, there are also exceptional cases of the fourfold accidental number degeneracy, for example, for $m = -11, n = -19$ and $m = -16, n = -17$. Pressure profiles of these four eigenmodes with the lowest frequency $\nu \approx 40$ are shown in the Appendix. Respectively, with opening of the triangular resonator with three attached waveguides these four eigenmodes are transformed into two superradiant modes and two FW BICs classified according to the two-dimensional irreducible representation E of group symmetry C_{3v}. Similar to open square resonator, only vertex attachment of waveguides allows the existence of degenerate BICs, as shown in Fig. 4. The resonant eigenmodes of the
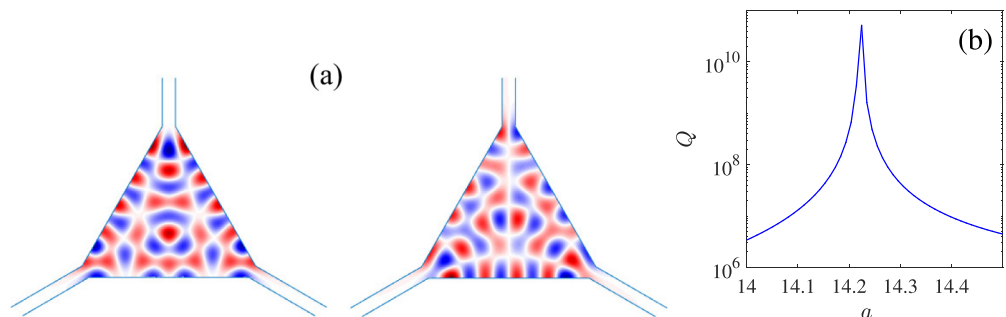
FIG. 4. (a) Degenerate BICs with the frequency $\nu_{BIC} = 0.8938$ classified according to the two-dimensional irreducible representation E of group symmetry C_{3v}. $a = a_c = 14.1939$. (b) The Q-factor dependence on side size of triangle a.
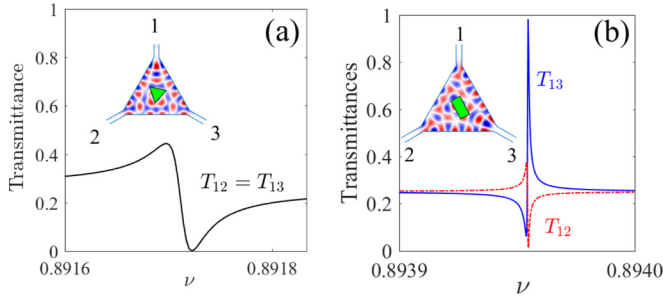
FIG. 5. Transmittance from input waveguide 1 into the output waveguides 2 and 3 in the triangular resonator with rotated (a) triangular pencil and (b) rectangular pencil. The frequency of input wave is tuned onto the frequency of degenerate FW BICs shown in Fig. 4.

open triangular resonator can be found only numerically as distinctive from the case of the square open resonator.

The existence of degenerate resonances and, in particular, BICs opens a way of highly effective manipulating out power flows by small perturbations. In particular, that can be done by slight violation of symmetry of the system, say, by slight local pressure onto the resonator walls. In the present paper, we apply a local perturbation in the form of pencil of triangular or rectangular cross sections at the center of the resonator which can be rotated by the angle θ relative to the resonator. Figure 5 demonstrates the striking result of the symmetry incompatibility of the resonator and perturbation. Figure 5(a) shows that perturbation which preserves the symmetry C_3 of the total system cannot manipulate by acoustic flows irrespective of the angle θ. However, the perturbation of the symmetry C_2 whose symmetry is not compatible with the symmetry of the total system drastically changes the output acoustic flows.

V. CONCLUSIONS

We considered square and triangular resonators with the symmetries whose eigenmodes are classified to the irreducible representations of group symmetries C_{4v} and C_{3v} among which there is the two-dimensional representation E. One can preserve the symmetries of open resonators owing to proper connection of waveguides to the resonator as sketched in Fig. 1. The Hamiltonian of closed resonator H_B transforms into non-Hermitian effective Hamiltonian H_{eff} after the Feshbach projection of the total system into space of eigenfunction of H_B [31]. Respectively, the eigenmodes of H_B with real eigenvalues are substituted by resonant modes, which are the eigenmodes of H_{eff} with complex eigenvalues. Both Hamiltonians commute with the symmetry group transformations, and therefore one can expect that there are twofold degenerate resonant states classified according to the two-dimensional irreducible representation E. However, analytical consideration in Sec. III explicitly shows these resonant states can not be true FW BICs because of the absence of interaction through the continuum of waveguides. In order to realize the degenerate FW BICs, we explore the unique property of square and triangular resonators of numeric accidental degeneracy of eigenmodes. As a result, we obtain the fourfold degeneracy of eigenmodes of H_B which transform into the twofold degenerate FW BICs and

two superradiant resonances. Shaw has presented even more unique cases of number eightfold degeneracy for $m = 5, n = 34$; $m = 10, n = 33$; $m = 13, n = 32$; $m = 24, n = 25$ with higher eigenfrequencies [22]. Respectively, we can expect the fourfold degenerate FW BICs or go above the first cutoff $\nu = 1$ towards the FW BICs embedded into a few continua of the next propagating bands of waveguides [38]. In general, degenerate BICs can also occur in open systems symmetrical, for example, relative to axial rotations. Then the Hilbert space of total system splits into a direct sum of spaces specified by the azimuthal index m. Respectively, the BICs, if they exist, are degenerate relative to $\pm m$ because of time-reversal symmetry. Examples of such degenerate BICs were reported in the periodical array of dielectric spheres [39] and disks [40]. However, these BICs are not degenerate in each Hilbert subspace specified by the azimuthal index m.

APPENDIX

1. The eigenmodes of square resonator classified according to irreducible representations of square symmetry group C_{4v}

In the acoustic square resonator with the Neumann boundary conditions result in the following eigenmodes

$$
\psi_{m,n}(x, y) = \sqrt{\frac{(2 - \delta_{m,1})(2 - \delta_{n,1})}{a}} \cos\left(\frac{\pi(m - 1)x}{a}\right)
$$
$$
\times \cos\left(\frac{\pi(n - 1)y}{a}\right) \tag{A1}
$$

with the eigenfrequencies

$$
\nu_{m,n}^2 = \omega_{m,n}^2/\omega_0^2 = (m - 1)^2 + (n - 1)^2, \, m, n = 1, 2, 3, \ldots, \tag{A2}
$$

where $\omega_0 = \pi s/a$, s is the velocity of sound in air and a is the size of square.

The group of symmetry C_{4v} of square consists of rotations C_4 and C_2, two mirror reflections σ_v along the square axis x and y and σ_v' along the diagonals of square [41,42]. Table I shows the irreducible representations of each symmetry transformation and their characters [42]. Fig. 6 shows that the eigenmodes $\psi_{m,2n+1}$ and $\psi_{2n+1,m}$ belong to the two-dimensional irreducible representation E. However, the eigenmodes $\psi_{2m,2m+2n}$ and $\psi_{2m+2n,2m}$ are classified by the reducible representations. As Fig. 7 shows, only the linear combinations $\psi_{2m+2n,2m} + \psi_{2m,2m+2n}$ and $\psi_{2m+2n,2m} - \psi_{2m,2m+2n}$ are classified according to the irreducible one-dimensional representations B_2 and A_2 respectively. Similarly, the linear combinations $\psi_{2m+2n+2,2m+1} + \psi_{2m+1,2m+2n+2}$ and

TABLE I. The characters of irreducible representations of group symmetry C_{4v}.

C_{4v}	1	C_2	$2C_4$	σ_x, σ_y	$\sigma_{xy}, \sigma_{xy}'$	basic modes
A_1	1	1	1	1	1	z
A_2	1	1	1	-1	-1	J_z
B_1	1	1	-1	1	-1	$x^2 - y^2$
B_2	1	1	-1	-1	1	xy
E	2	-2	0	0	0	x, y
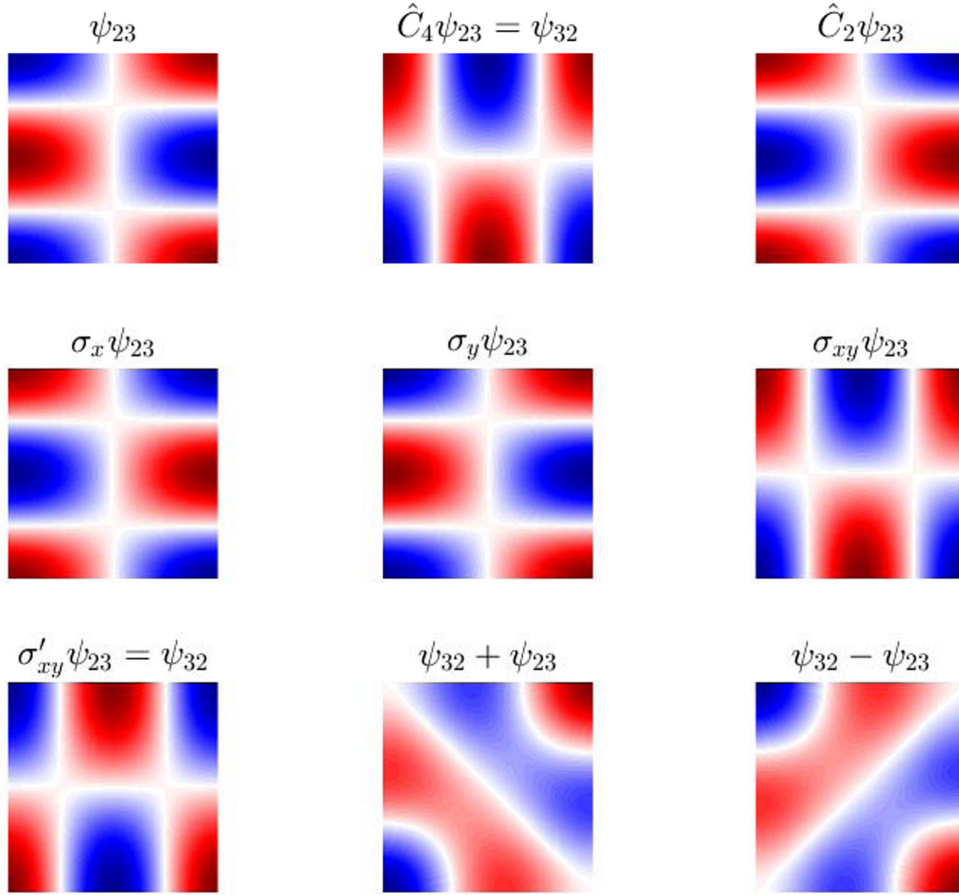
FIG. 6. Symmetry group C_{4v} transformations of the eigenmode $\psi_{23}(x, y)$.

$\psi_{2m+2n+2,2m+1} - \psi_{2m+1,2m+2n+2}$ are classified according to the irreducible one-dimensional representations B_1 and A_1 respectively. In Fig. 8 we present an example of eigenmodes ψ_{16} and ψ_{54} degenerated accidentally [22,23].

2. Effective non-Hermitian Hamiltonian

The procedure of the Feshbach projection of the total Hilbert space of the total system closed resonator plus waveguides with Neumann boundary conditions onto Hilbert space of the eigenmodes of closed resonator is described in Ref. [36]. In application to the square acoustic resonator we have

$$\widehat{H}_{\text{eff}} = v_{mn}^2 \delta_{mm'} \delta_{nn'} - \sum_{p=1}^{\infty} \sum_{C} i k_p \widehat{W}_{Cp} \widehat{W}_{Cp}^{\dagger}, \quad \text{(A3)}$$

where k_p are the propagating momenta of the pth channel in waveguides of width d. In what follows, all dimensions are measured in terms of d, i.e., $d = 1$. Then

$$v^2 = k_p^2 + (p - 1)^2, \quad p = 1, 2, 3, \dots \quad \text{(A4)}$$

with

$$\phi_p(x, y) = \sqrt{2 - \delta_{p,1}} \cos(\pi (p - 1) y) e^{i k_p x}. \quad \text{(A5)}$$

The index w in Eq. (A3) sorts waveguides. For attachments of waveguides shown in Fig. 1 of the main text the coupling matrix $\widehat{W}_{Cp}$ can be evaluated analytically

$$W_{mn;p,C=1,3} = \int_{-1/2}^{1/2} \psi_{mn}(x = \mp a/2, y) \phi_p(y) dy, \quad \text{(A6)}$$

$$W_{mn;p,C=2,4} = \int_{-1/2}^{1/2} \psi_{mn}(x, y = \pm a/2) \phi_p(x) dx. \quad \text{(A7)}$$

After integration in geometry shown in Fig. 1(b) of the paper we obtain for the waveguide 1:

$$W_{mn;p,C=1} = \frac{\sqrt{(2 - \delta_{m,1})(2 - \delta_{n,1})(2 - \delta_{p,1})}}{\pi} \left[\frac{\sin\left[\frac{\pi}{2a}(n - 1 + a(p - 1))\right] \cos\left[\frac{\pi}{2}(n - 1 + a(p - 1))\right]}{n - 1 + a(p - 1)} \right.$$
$$\left. + \frac{\sin\left[\frac{\pi}{2a}(n - 1 - a(p - 1))\right] \cos\left[\frac{\pi}{2}(n - 1 - a(p - 1))\right]}{n - 1 - a(p - 1)} \right\}. \quad \text{(A8)}$$
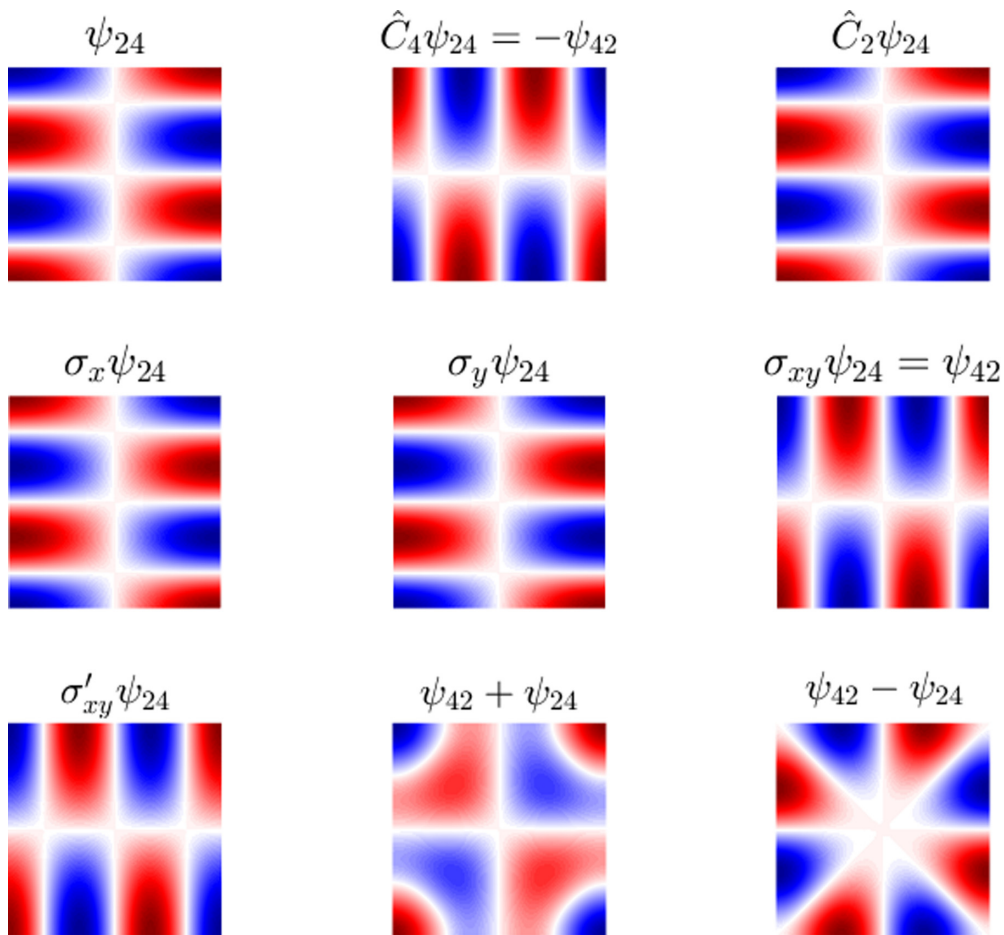
FIG. 7. Symmetry group C_{4v} transformations for the eigenmode $\psi_{24}(x, y)$.

FIG. 8. The number degenerated eigenfunctions of square.

Some particular coupling matrix elements relevant for the paper are collected in Tables II and III where according to Eq. (A8) we denote

$$b(a) = \frac{4\sqrt{2}a}{\pi(a^2 - 9)} \sin \frac{\pi a}{2} \cos \frac{3\pi}{2a},$$

$$c(a) = \frac{4\sqrt{2}a}{\pi(a^2 - 4)} \sin \frac{\pi a}{2} \cos \frac{\pi}{2a},$$

$$f(a) = \frac{4\sqrt{2}a}{\pi(a^2 - 4)} \cos \frac{\pi}{a} \cos \frac{\pi a}{2},$$

TABLE II. Coupling matrix elements with the first open channel $p = 1$.

modes $m, n \setminus C$	1	2	3	4
2, 3	$-\frac{2}{\pi} \sin \frac{\pi}{a}$	0	$\frac{2}{\pi} \sin \frac{\pi}{a}$	0
3, 2	0	$\frac{2}{\pi} \sin \frac{\pi}{a}$	0	$-\frac{2}{\pi} \sin \frac{\pi}{a}$
2, 4	0	0	0	0
4, 2	0	0	0	0
1, 6	0	$\frac{\sqrt{2}}{a}$	0	$-\frac{\sqrt{2}}{a}$
5, 4	0	$\frac{1}{\pi} \sin \frac{2\pi}{a}$	0	$-\frac{1}{\pi} \sin \frac{2\pi}{a}$
6, 1	$\frac{\sqrt{2}}{a}$	0	$-\frac{\sqrt{2}}{a}$	0
4, 5	$\frac{1}{\pi} \sin \frac{2\pi}{a}$	0	$-\frac{1}{\pi} \sin \frac{2\pi}{a}$	0

TABLE III. Coupling matrix elements with the second closed channel $p = 2$.

modes $m, n \setminus C$	1	2	3	4
2, 3	0	$-f(a)$	0	$f(a)$
3, 2	$-f(a)$	0	$f(a)$	0
2, 4	$-b(a)$	$-c(a)$	$b(a)$	$c(a)$
4, 2	$c(a)$	$b(a)$	$-c(a)$	$-b(a)$
1, 6	$g(a)$	0	$g(a)$	0
5, 4	$-h(a)$	0	$-h(a)$	0
6, 1	0	$g(a)$	0	$g(a)$
4, 5	0	$h(a)$	0	$h(a)$

$$g(a) = -\frac{4a}{\pi(a^2 - 25)} \cos \frac{5\pi}{2a} \sin \frac{\pi a}{2},$$

$$h(a) = \frac{4\sqrt{2}a}{\pi(a^2 - 16)} \cos \frac{2\pi}{a} \cos \frac{\pi a}{2}. \quad \text{(A9)}$$

3. Eigenmodes of equilateral triangular billiard

The eigenfrequencies of equilateral triangle equal for the Neumann boundary conditions

$$\nu_{mn}^2 = \omega_{mn}^2 / \omega_0^2$$
$$= \frac{16}{27}(m^2 + n^2 - mn), m, n = 0, \pm 1, \pm 2, \dots, \quad \text{(A10)}$$

where ω_0 is defined in Eq. (A2) with the following conditions: $m + n$ is a multiple of 3 [43]. The eigenmodes are of the form

$$\psi_{mn} = f_{mn} + f_{m,m-n} + f_{-n,m-n} + f_{-n,-m}$$
$$+ f_{n-m,-m} + f_{n-m,n}$$
$$f_{mn}(x, y) = \exp(2\pi i/3)(nx + (2n - m)y/\sqrt{3}). \quad \text{(A11)}$$

In Fig. 9 we show patterns of the eigenmodes which are fourfold degenerate due to permutation symmetry $m \leftrightarrow n$ and accidental number degeneracy at $m = -16, n = -17$ and $m = 11, n = -19$.
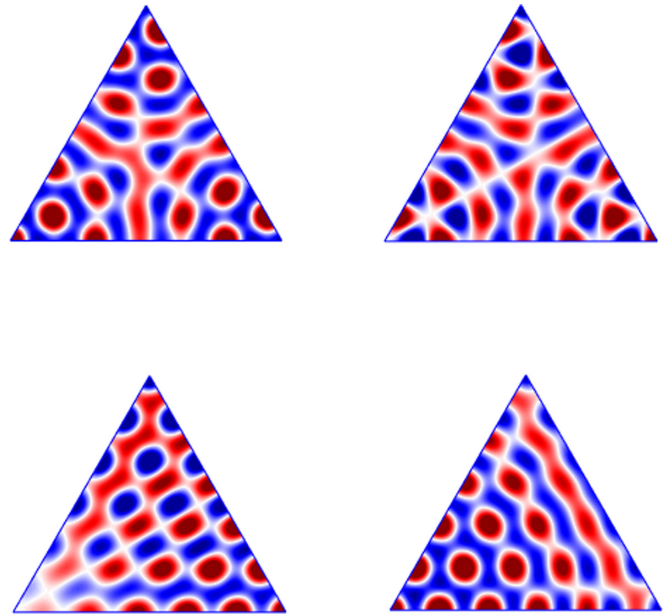
FIG. 9. Fourfold degenerate eigenvalues of equilateral triangle with eigenfrequencies $\nu_{-11,-19}^2 = \nu_{-16,-17}^2 = 161.778$.

There are also other cases of the fourfold degeneracy however with higher eigenfrequencies with $m = -13, n = -23, m = -23, n = -13$ and $m = -17, n = -22, m = -22, n = -17$ with the eigenvalue $\nu_{13,-23}^2 = 226.312$. The group of symmetry C_{3v} of equilateral triangle consists of rotations C_3, mirror reflections σ_v along the diagonals of resonator [42]. Table IV shows the irreducible representations of each symmetry transformation and their characters [42].

TABLE IV. The characters of irreducible representations of group symmetry C_{3v}.

C_{3v}	1	$2C_3$	$3\sigma_v$	basic modes
A_1	1	1	1	z
A_2	1	1	-1	J_z
E	2	-1	0	x, y

[1] Chia Wei Hsu, Bo Zhen, A. D. Stone, J. D. Joannopoulos, and M. Soljačić, Bound states in the continuum, Nat. Rev. Mater. **1**, 16048 (2016).

[2] G. Quaranta, G. Basset, O. J. F. Martin, and B. Gallinet, Recent advances in resonant waveguide gratings, Laser Photonics Rev. **12**, 1800017 (2018).

[3] L. Huang, L. Xu, M. Woolley, and A. E. Miroshnichenko, Trends in quantum nanophotonics, Adv. Quantum Technol. **3**, 1900126 (2020).

[4] A. F. Sadreev, Interference traps waves in an open system: bound states in the continuum, Rep. Prog. Phys. **84**, 055901 (2021).

[5] S. Joseph, S. Pandey, S. Sarkar, and J. Joseph, Bound states in the continuum in resonant nanostructures: an overview of engineered materials for tailored applications, Nanophotonics **10**, 4175 (2021).

[6] M. Bolsterli, Continuity of phase shift at continuum bound state, Phys. Rev. **182**, 1095 (1969).

[7] M. Robnik, A simple separable Hamiltonian having bound states in the continuum, J. Phys. A: Math. Gen. **19**, 3845 (1986).

[8] R. L. Schult, D. G. Ravenhall, and H. W. Wyld, Quantum bound states in a classically unbound system of crossed wires, Phys. Rev. B **39**, 5476 (1989).

[9] D. Evans and R. Porter, Trapped modes embedded in the continuous spectrum, Q. J. Mech. Appl. Math. **51**, 263 (1998).

[10] N. Moiseyev, Suppression of Feshbach Resonance Widths in Two-Dimensional Waveguides and Quantum Dots: A Lower

Bound for the Number of Bound States in the Continuum, Phys. Rev. Lett. **102**, 167404 (2009).

[11] H. Friedrich and D. Wintgen, Interfering resonances and bound states in the continuum, Phys. Rev. A **32**, 3231 (1985).

[12] A. F. Sadreev, E. N. Bulgakov, and I. Rotter, Bound states in the continuum in open quantum billiards with a variable shape, Phys. Rev. B **73**, 235342 (2006).

[13] C. Linton, M. McIver, P. McIver, K. Ratcliffe, and J. Zhang, Trapped modes for off-centre structures in guides, Wave Motion **36**, 67 (2002).

[14] Y. Duan, W. Koch, C. Linton, and M. McIver, Complex resonances and trapped modes in ducted domains, J. Fluid Mech. **571**, 119 (2007).

[15] S. Hein and W. Koch, Acoustic resonances and trapped modes in pipes and tunnels, J. Fluid Mech. **605**, 401 (2008).

[16] A. A. Lyapina, D. N. Maksimov, A. S. Pilipchuk, and A. F. Sadreev, Bound states in the continuum in open acoustic resonators, J. Fluid Mech. **780**, 370 (2015).

[17] S. Huang, T. Liu, Z. Zhou, X. Wang, J. Zhu, and Y. Li, Extreme Sound Confinement from Quasibound States in the Continuum, Phys. Rev. Applied **14**, 021001 (2020).

[18] T. Lepetit and B. Kanté, Controlling multipolar radiation with symmetries for electromagnetic bound states in the continuum, Phys. Rev. B **90**, 241103(R) (2014).

[19] L. Huang, Y. K. Chiang, S. Huang, C. Shen, F. Deng, Y. Cheng, B. Jia, Y. Li, D. A. Powell, and A. E. Miroshnichenko, Sound trapping in an open resonator, Nat. Commun. **12**, 4819 (2021).

[20] A. Volya and V. Zelevinsky, Non-hermitian effective Hamiltonian and continuum shell model, Phys. Rev. C **67**, 054322 (2003).

[21] A. Lyapina, A. Pilipchuk, and A. Sadreev, Trapped modes in a non-axisymmetric cylindrical waveguide, J. Sound Vib. **421**, 48 (2018).

[22] G. B. Shaw, Degeneracy in the particle in a box problem, J. Phys. A: Math. Nucl. Gen. **7**, 1537 (1974).

[23] J. R. Kuttler and V. G. Sigillito, Eigenvalues of the laplacian in two dimensions, SIAM Rev. **26**, 163 (1984).

[24] S. Gladyshev, K. Frizyuk, and A. Bogdanov, Symmetry analysis and multipole classification of eigenmodes in electromagnetic resonators for engineering their optical properties, Phys. Rev. B **102**, 075103 (2020).

[25] L. Huang, L. Xu, M. Rahmani, D. Neshev, and A. Miroshnichenko, Pushing the limit of high-Q mode of a single dielectric nanocavity, Adv. Photonics **3**, 016004 (2021).

[26] K. Pichugin, A. Sadreev, and E. Bulgakov, Ultrahigh-Q system of a few coaxial disks, Nanophotonics **10**, 4341 (2021).

[27] A. Overvig, S. Malek, M. Carter, S. Shrestha, and N. Yu, Selection rules for quasibound states in the continuum, Phys. Rev. B **102**, 035434 (2020).

[28] A. Overvig, N. Yu, and A. Alù, Chiral Quasi-Bound States in the Continuum, Phys. Rev. Lett. **126**, 073001 (2021).

[29] V. Dmitriev, A. Kupriianov, S.D.S.S., and V. Tuz, Symmetry analysis of trimer-based all-dielectric metasurfaces with toroidal dipole modes, J. Phys. D: Appl. Phys. **54**, 115107 (2021).

[30] M. Tsimokha, V. Igoshin, A. Nikitina, I. Toftul, K. Frizyuk, and M. Petrov, Acoustic resonators: Symmetry classification and multipolar content of the eigenmodes, Phys. Rev. B **105**, 165311 (2022).

[31] H. Feshbach, Unified theory of nuclear reactions, Ann. Phys. **5**, 357 (1958).

[32] H. Feshbach, A unified theory of nuclear reactions. II, Ann. Phys. **19**, 287 (1962).

[33] I. Rotter, A continuum shell model for the open quantum mechanical nuclear system, Rep. Prog. Phys. **54**, 635 (1991).

[34] F. Dittes, The decay of quantum systems with a small number of open channels, Phys. Rep. **339**, 215 (2000).

[35] A. Sadreev and I. Rotter, S-matrix theory for transmission through billiards in tight-binding approach, J. Phys. A: Math. Gen. **36**, 11413 (2003).

[36] D. N. Maksimov, A. F. Sadreev, A. A. Lyapina, and A. S. Pilipchuk, Coupled mode theory for acoustic resonators, Wave Motion **56**, 52 (2015).

[37] R. Kikkawa, M. Nishida, and Y. Kadoya, Polarization-based branch selection of bound states in the continuum in dielectric waveguide modes anti-crossed by a metal grating, New J. Phys. **21**, 113020 (2019).

[38] F. Remacle, M. Munster, V. Pavlov-Verevkin, and M. Desouter-Lecomte, Trapping in competitive decay of degenerate states, Phys. Lett. A **145**, 265 (1990).

[39] E. N. Bulgakov and A. F. Sadreev, Light trapping above the light cone in a one-dimensional array of dielectric spheres, Phys. Rev. A **92**, 023816 (2015).

[40] E. N. Bulgakov and A. F. Sadreev, Bound states in the continuum with high orbital angular momentum in a dielectric rod with periodically modulated permittivity, Phys. Rev. A **96**, 013841 (2017).

[41] L. D. Landau and E. M. Lifshitz, *Quantum Mechanics: Nonrelativistic Theory. V. 3 of Course of Theoretical Physics* (Pergamon Press, 1958).

[42] G. L. Bir and G. E. Pikus, *Symmetry and Strain-Induced Effects in Semiconductors* (Wiley New York, 1974).

[43] M. A. Pinsky, The eigenvalues of an equilateral triangle, SIAM J. Math. Anal. **11**, 819 (1980).